Synchrotron X-ray studies of metal-organic framework M_2(2,5-dihydroxyterephthalate), M = (Mn, Co, Ni, Zn) (MOF74)

W. Wong-Ng,[1,a)] J. A. Kaduk,[2] H. Wu,[1] and M. Suchomel[3]
[1]*National Institute of Standards and Technology, Gaithersburg, Maryland 20899*
[2]*Illinois Institute of Technology, Chicago, Illinois 60616*
[3]*Advanced Photon Source, Argonne National Laboratory, Argonne, Illinois 60439-4856*

(Received 6 July 2012; accepted 2 October 2012)

M_2(dhtp)·nH$_2$O (M = Mn, Co, Ni, Zn; dhtp = 2,5-dihydroxyterephthalate), known as MOF74, is a family of excellent sorbent materials for CO_2 that contains coordinatively unsaturated metal sites and a honeycomb-like structure featuring a broad one-dimensional channel. This paper describes the structural feature and provides reference X-ray powder diffraction patterns of these four isostructural compounds. The structures were determined using synchrotron diffraction data obtained at beam line 11-BM at the Advanced Photon Source (APS) in the Argonne National Laboratory. The samples were confirmed to be hexagonal R $\bar{3}$ (No. 148). From M = Mn, Co, Ni, to Zn, the lattice parameter a of MOF74 ranges from 26.131 73(4) Å to 26.5738(2) Å, c from 6.651 97(5) to 6.808 83(8) Å, and V ranges from 3948.08 Å^3 to 4163.99 Å^3, respectively. The four reference X-ray powder diffraction patterns have been submitted for inclusion in the Powder Diffraction File (PDF). © *2012 International Centre for Diffraction Data.* [doi:10.1017/S0885715612000863]

Key words: Metal-organic framework, MOF74, M_2(2,5-dihydroxyterephthalate)·nH$_2$O, (M = Mn, Co, Ni, Zn), Synchrotron X-ray, High resolution diffraction patterns

I. INTRODUCTION

In recent years, a considerable surge of attention to the porous metal-organic framework (MOF) materials was due to their potential applications in both H_2 storage and CO_2 capture. However, most MOF materials have low thermal stability as compared to zeolites. Often, one needs to remove solvent or other guest molecules from the pores at elevated temperature, leading to the instability of the framework structure. Therefore, it is important to seek materials with structural stability at elevated temperature. The 'dhtp' linker (dhtp = 2,5-dihydroxytetephthalate or 2,5-dihydroxy-1,4-benzenedicarboxylate) is known to form microporous coordination polymers based on the dianionic form of the carboxyl moieties which act as ligands to metal sites. The M^{II}_2(dhtp) compounds, also known as the MOF74 family (Rosi *et al.*, 2005), demonstrated stability even after the removal of coordinated water (Dietzel *et al.*, 2005).

Extensive research has been performed on the MOF74 family of materials since the first report by Rosi *et al.* (2005) on the synthesis and characterization of the Zn-MOF74 analog. For example, Dietzel *et al.* (2005) carried out an *in situ* high-temperature single-crystal investigation of Co-MOF74 and hydrogen adsorption studies using Ni-MOF74 (Dietzel, 2006). Caskey *et al.* (2008) reported the dramatic tuning of CO_2 uptake in the Mg-, Ni-, Co-, and Zn-MOF74 compounds. In the same year, Tranchemontagne *et al.* (2008) reported for the first time the room temperature synthesis of Zn-MOF74, and Zhou *et al.* (2008), combining experimental with theoretical efforts, showed that the enhanced H_2 adsorption in M-MoF74 (M = Mg, Mn, Co, Ni, Zn) has a strong dependence of the binding strength on the open metal sites. In the following year, Wu *et al.* (2009) illustrated the important role of open metal sites for high-capacity methane storage. As selective binding of CO_2 is essential for CO_2 capture and natural gas purification, Britt *et al.* (2009) using the Mg-analog show CO_2 release at a temperature as low as 80 °C. Wu *et al.* (2010) further explored the adsorption sites and binding nature of CO_2 in Mg-MOF74 using a combined neutron diffraction and first-principles study. Glover *et al.* (2011) extended the capability of M-MOF74 (M = Mg, Zn, Co, Ni) to the removal of ammonia, cyanogen chloride, and sulfur dioxide from air.

In addition to thermal stability, the MOF74 family of materials also has record setting surface areas coupled with high free volumes. For example, the Mg materials have 8.9 wt% dynamic capacity and exhibit facile CO_2 release at a significantly low temperature of 80 °C (Britt *et al.*, 2009). These compounds are also effective sorbents in the low pressure region (0 to 101.3 kPa) for CO_2 uptake. Therefore, MOF74 offers a balance between dynamic capacity and regeneration.

As X-ray powder diffraction is a non-destructive method for characterization, X-ray reference diffraction patterns for sorbent materials play an important role for the research community that investigates efficient solid sorbent materials for the CO_2 capture process. The goal of this report is two-fold: a brief comparison of the structural features of the MOF74 (M = Mn, Co, Ni, Zn) members, and the determination of their high resolution experimental powder diffraction patterns for inclusion in the Powder Diffraction File (PDF).

a) Author to whom correspondence should be addressed. Electronic mail: winnie.wong-ng@nist.gov

II. EXPERIMENTAL[1]

Details of the synthesis of the MOF74 samples were reported elsewhere (Zhou *et al.*, 2008 and references cited in the Supporting Information). Sample loading into the capillaries used for data collection was performed inside a dry box with flowing Ar at room temperature.

High resolution synchrotron X-ray powder diffraction data MOF74 (Mn, Co, Ni, and Zn) were collected at 293 K using beamline 11-BM at the Advanced Photon Source (APS), Argonne National Laboratory using an average wavelength of 0.412 210 Å. Discrete detectors covering an angular range from −6° to 16° with respect to the nominal 2θ were scanned over a 34°2θ range, with data points collected every 0.001° in 2θ at a scan speed of 0.01°/s. The instrumental optics of 11-BM incorporate two platinum-striped mirrors and a double-crystal Si(111) monochromator, where the second crystal has an adjustable sagittal bend (Wang *et al.*, 2008). The diffractometer is controlled via EPICS (Dalesio *et al.*, 1994). A vertical Huber 480 goniometer positions 12 perfect Si(111) analyzers and 12 Oxford-Danfysik $LaCl_3$ scintillators, with a spacing of 2° in 2θ (Lee *et al.*, 2008). Capillary samples are mounted by a robotic arm and spun at ≈90 Hz. Data are normalized to incident flux and collected while continually scanning the diffractometer 2θ arm. A mixture of National Institute of Standards and Technology standard reference materials, Si (SRM^{TM} 640c) and Al_2O_3 (SRM^{TM} 676) is used to calibrate the instrument, where the Si lattice constant determines the wavelength for each detector. Corrections are applied for detector sensitivity, 2θ offset, and small detector wavelength differences, before merging the data into a single set of intensities evenly spaced in 2θ.

The high-resolution patterns of MOF74 were fitted using the Rietveld refinement technique (Rietveld, 1969) with the software suite GSAS (Larson and von Dreele, 1992). For M = Mn, Ni, and Zn, the $C_8H_2O_6$ dhtp ligand was modeled as a rigid body of half-occupied atoms, with the center of the molecule fixed at the inversion center 1/3, 1/6, 1/6 and only the three orientation angles refined. For M = Co, the C_8H_2 core of the dhtp ligand was modeled as a rigid body of half-occupied atoms, and distance and angle restraints were applied to the carboxyl and ionized hydroxyl groups. The peak profiles were described using the aniosotropic strain tensor model of GSAS profile function #4. Preferred orientation was modeled using fourth-order spherical harmonics; the texture index varied from 1.015 to 1.128. The background was modeled using a three-term shifted Chebyshev function, and 9–14-term diffuse scattering functions were also included.

The reference X-ray powder patterns were obtained with a Rietveld pattern decomposition technique. In this technique, the reported peak positions are derived from the extracted integrated intensities and positions calculated from the lattice parameters. When peaks are not resolved at the resolution function of the diffractometer, the intensities are summed, and an intensity-weighted d-spacing is reported. Therefore, these patterns represent ideal specimens. They are corrected for systematic errors both in d-spacing and intensity.

[1] The purpose of identifying the chemical and equipment in this article is to specify the experimental procedure. Such identification does not imply recommendation or endorsement by the National Institute of Standards and Technology.

III. RESULTS AND DISCUSSION

A. Crystal structure

Figures 1(a)–1(d) show the results of the synchrotron Rietveld refinement of Mn-, Co-, Ni-, and Zn-MOF74 samples. Tick marks indicate peak positions. The difference pattern is plotted on the same scale as the other patterns. In these diagrams, for 2θ values higher than 4°, the scale has been magnified 20 times. At 2θ values are higher than 13°, the scale has been magnified 50 times. The refinement results of the four samples are listed in Table I. No significant impurity phase was found in these samples. Despite the fact that after the samples was loaded into the capillary tubings and was sealed with wax, moisture apparently diffuses into the tubings. The final chemical formula for these compounds was estimated to be $[M_2(C_8H_2O_6)(H_2O)_2]\cdot nH_2O$, where n = 6.3, 10.0, 6.2, and 6.6 for M = Mn, Co, Ni, Zn. Owing to the disordered situation of water molecules, no attempts were made to locate the hydrogen atoms in the pores.

Based on the refinement results, the MOF74 samples are isostructural and the space group was confirmed to be R $\bar{3}$ (No. 148). Table II gives the cell parameters of these phases, and the calculated densities of these phases. The much higher density value for the Co-phase is attributed to the higher number of water molecules in the channels as compared to the remaining three samples. The ionic radii (Shannon, 1976) for Ni^{2+}(VI), Zn^{2+}(VI), Co^{2+}(VI), and Mn^{2+}(VI) are 0.69 Å, 0.74 Å, 0.745 Å, and 0.83 Å, respectively. As Mn^{2+} has a larger size, it is expected to have larger lattice parameters. The trend of the unit cell volume in Table II follows the trend of the ionic radius of the cations.

Table III gives the atomic coordinates of the four MOF74 materials. Figures 2 and 3 depict the crystal structure of Zn and Co compounds featuring a three-dimensional coordination polymer with honeycomb topology that contains one-dimensional broad channels. The M-atoms are coordinated in a distorted octahedral fashion by six oxygen atoms. Five of the six oxygen atoms are part of the organic ligand. The sixth one comes from a coordinated water molecule (O18 in the numbering scheme). In general, the pores of the as-synthesized material are occupied with solvent molecules such as H_2O which can be removed upon evacuation to generate unsaturated metal sites. Therefore, the coordination number around the M depends on whether the sample is hydrated or not (distorted octahedral or square pyramid, respectively). In the anhydrous state, MOF74 contains open metal sites that are known to play a vital role in enhanced bonding of various gas molecules (H_2, CH_4, C_2H_2, NO, CO_2, etc.) (Wu *et al.* 2010). In Figures 2 and 3, only the oxygen atoms of the water molecules are shown. The channels in the honeycomb have a diameter of about 11 Å. The main difference between the Co-analog and the other three is the different number of adsorbed H_2O molecules. For example, Co-MOF74 has about 10 water molecules per formula while the other three samples with M = Mn, Ni and Zn have around 6–7. As these three metals have the same charge in the same structure, the polarity/hydrophilicity of the frameworks can be reasonably expected to be similar, and thus the water contents are similar. In Table III, water molecules of hydration are included in the formula. In Mn-MOF74 and Ni-MOF74, O19 of the water molecule is situated on a three-fold axis whereas in Co-MOF74 and Zn-MOF74, no water molecule occupies a

https://doi.org/10.1017/S0885715612000863 Published online by Cambridge University Press

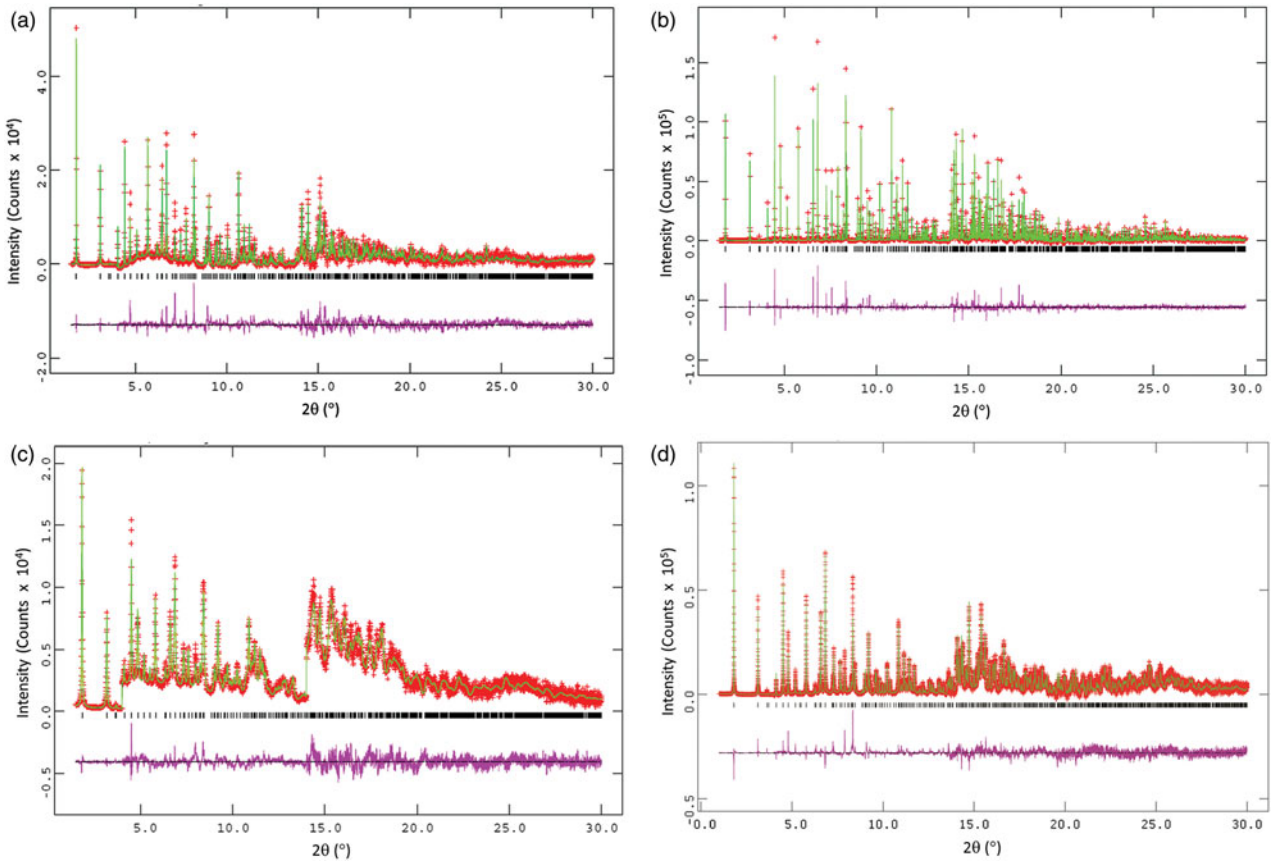

Figure 1. Rietveld refinement results for (a) M_2(dhtp), M=Mn; (b) M_2(dhtp), M = Co; (c) M_2(dhtp), M = Ni; (d) M_2(dhtp), M = Zn. The row of tick marks indicates the calculated peak positions. The difference pattern is plotted at the same scale as the other patterns up to 5° in 2θ. At 5° 2θ, the scale has been magnified 20 times. At 2θ values greater than 13.5°, the scale has been magnified 50 times.

TABLE I. Rietveld refinement results for M_2(dhtp), M = Mn, Co, Ni, Zn (λ = 0.413 535 Å)

	χ2	No. of parameters	R	wR
Mn	3.311	39	0.0617	0.0791
Co	7.954	81	0.1097	0.1310
Ni	1.970	41	0.0588	0.0759
Zn	3.544	56	0.0706	0.0843

three-fold axis. The resulting formulae are $M_6(C_{24}H_6O_{18})(H_2O)_6],\cdot 3nH_2O$ (Z = 3, M = Mn, Ni,), and $M(C_4HO_3)(H_2O)\cdot nH_2O$ (Z = 18, M = Co and Zn).

Table IV gives the pertinent M–O bond distances in the four MOF74 analogs, respectively. The MO_6 groups are shown as having a distorted octahedral environment, and the degree of distortion of the MO_6 octahedra is similar. In the four MOF74 compounds, four of the M–O distances are shorter than the other two. The water molecule (M–O18) is *trans* to the longest M–O bond, and its M–O18 distance is also elongated. The distorted geometry of the octahedron is also illustrated by the O–M–O angles. In these compounds, the distorted angles range from 84.7(3)° to 101.5(3)° in the Mn-analog, from 81.8(2)° to 95.8(2)° in the Co-analog, from 73.36(10)° to 103.3(2)° in the Ni-analog, and from 75.00(8)° to 103.10(10)° in the Zn-analog.

The bond valence sum values, V_b, for M–O distances were calculated using the Brown–Altermatt empirical expression (Brown and Altermatt, 1985; Brese and O'Keeffe, 1991). The V_b of an atom i is defined as the sum of the bond valences v_{ij} of all the bonds from atoms i to atoms j. The most commonly adopted empirical expression for bond valence v_{ij} as a function of the interatomic distance d_{ij} is $v_{ij} = \exp[(R_0 - d_{ij})/B]$. The parameter, B, is commonly taken to be a "universal" constant equal to 0.37 Å. The values for the reference distance R_0 for Mn^{II}–O, Co^{II}–O, Ni^{II}–O, and Zn^{II}–O are 1.790, 1.692, 1.654, and 1.704 respectively (Brown and Altermatt, 1985; Brese and O'Keeffe, 1991).

TABLE II. Cell parameters for M_2(dhtp) (M=Mn, Co, Zn, Ni); space group $R\bar{3}$, Z = 3

M	a (Å)	c (Å)	V(Å^3)	D_x
Mn	26.5738(2)	6.808 83(8)	4163.99(6)	1.569
Co	26.131 73(4)	6.722 02(1)	3975.28(1)	1.896
Zn	26.178 97 (10)	6.651 97(5)	3948.08(4)	1.750
Ni	25.8561(4)	6.7119(2)	3885.98(1)	1.702

https://doi.org/10.1017/S0885715612000863 Published online by Cambridge University Press

TABLE III. Atomic coordinates and displacement factors (U_{iso}) for M_2(dhtp); space group R $\bar{3}$. In this table, water molecules of hydration are included in the formula. The resulting formulae are $M_6(C_{24}H_6O_{18})(H_2O)_6]\cdot 3nH_2O$ (Z = 3, *M*=Mn, Ni,), or $M(C_4HO_3)(H_2O)\cdot nH_2O$ (Z = 18, *M* = Co and Zn). SOF represents the site occupancy factor.

Atom	*x*	*y*	*Z*	SOF	U_{iso}
(1) *M*=Mn; $[Mn_6(C_{24}H_6O_{18})(H_2O)_6\cdot 18.9H_2O$; Z = 3]					
Mn1	0.390 72(9)	0.351 77(9)	0.1430(3)	1.0	0.0067(5)
C2	0.321 25(7)	0.201 73(5)	0.2866(2)	1.0	0.009(2)
C3	0.338 97(9)	0.218 15(5)	0.0934(2)	1.0	0.009
C4	0.351 06(11)	0.183 09(8)	−0.026 56(12)	1.0	0.009
H8	0.3648(2)	0.1958(2)	−0.1776(2)	1.0	0.0121
C10	0.3082(2)	0.2394(1)	0.4157(4)	1.0	0.027(2)
O11	0.3133(2)	0.285 85(11)	0.3496(6)	1.0	0.027
O12	0.2923(2)	0.2246(2)	0.5899(4)	1.0	0.027
O16	0.3444(2)	0.26 801(10)	0.0225(5)	1.0	0.027
O18	0.2213(4)	0.2079(4)	−0.0264(14)	1.0	0.124
Oxygens (of water molecules in channels, hydrogens not located)					
O19	0.333 33	0.666 67	0.166 67	1.0	0.124
O20	0.4685(4)	0.1120(4)	−0.0301(15)	1.0	0.124
O21	0.0540(4)	0.0031(6)	0.2142(14)	1.0	0.124
O22	0.2759(6)	0.4938(4)	0.152(2)	1.0	0.124
(2) M = Co; $[Co(C_4HO_3)(H_2O)\cdot 4.9H_2O$; Z = 18]					
Co1	0.384 96(5)	0.349 26(5)	0.150 08(14)	1.0	0.0157(3)
C2	0.3293(3)	0.2081 (2)	0.2854(7)	1.0	0.0197(13)
C3	0.3442(3)	0.2202(13)	0.0852(7)	1.0	0.0197(13)
C4	0.3482(2)	0.1787(2)	−0.0335(2)	1.0	0.0197(13)
H8	0.3598(4)	0.1880(4)	−0.1889(4)	1.0	0.026(2)
C10	0.3139(3)	0.2456(3)	0.4230(8)	1.0	0.0177(8)
O11	0.3238(2)	0.2920(2)	0.3584(6)	1.0	0.0177(8)
O12	0.2997(2)	0.2289(2)	0.5902(7)	1.0	0.0177(8)
O16	0.3554(2)	0.2721(2)	−0.0043(7)	1.0	0.0177(8)
O18	0.2181(2)	0.2119(2)	−0.0410(6)	1.0	0.032(2)
Oxygens (of water molecules in channels, hydrogens not located)					
O20	0.4816(4)	0.1179(4)	−0.0061(14)	1.0	0.158 (3)
O21	0.0463(11)	−0.0290(12)	0.446(4)	0.470(9)	0.158 (3)
O22	0.1691(5)	0.5564(5)	0.137(2)	1.0	0.158 (3)
O23	0.1563(6)	0.0755(5)	0.183(2)	0.748(11)	0.158 (3)
O24	0.4184(7)	0.5574(9)	0.690(3)	0.560(11)	0.158 (3)
O26	0.2815(6)	0.6575(8)	0.535(2)	0.629(8)	0.158 (3)
O27	0.1491(8)	0.5427(8)	0.924(2)	0.609(14)	0.158 (3)
(3) M = Ni; $[Ni_6(C_{24}H_6O_{18})(H_2O)_6\cdot$ 18.6H_2O; Z = 3]					
Ni1	0.383 77(8)	0.348 87(7)	0.1445 (2)	1.0	0.0008(5)
C2	0.323 25(7)	0.204 45(5)	0.287 77(16)	1.0	0.02
C3	0.336 07(10)	0.217 63(6)	0.0865 (2)	1.0	0.02
C4	0.346 15(12)	0.179 85(9)	−0.0346(1)	1.0	0.02
H8	0.3561(2)	0.1901(2)	−0.190 89(17)	1.0	0.026
C10	0.3124(2)	0.245 08(11)	0.4180 (3)	1.0	0.02
O11	0.3149(2)	0.291 03(11)	0.3457(5)	1.0	0.02
O12	0.3009(2)	0.2332(2)	0.5995(3)	1.0	0.02
O16	0.3387(2)	0.266 99(12)	0.0089(4)	1.0	0.02
O18	0.2272	0.1874	−0.0828	1.0	0.184(4)
Oxygens (of water molecules in channels, hydrogens not located)					
O19	0.333 33	0.666 67	0.166 67	0.55(4)	0.184
O20	0.4728(6)	0.1165(5)	−0.0594(15)	1.0	0.184
O21	0.0835(7)	0.0519(6)	0.2535(19)	1.0	0.184
O22	0.1691(6)	0.0599(6)	0.0318(17)	1.0	0.184
(4) M = Zn; $[Zn(C_4HO_3)(H_2O)\cdot$ 3.3H_2O; Z = 18]					
Zn1	0.387 90(5)	0.350 69(5)	0.1522(2)	1.0	0.0134(3)
C2	0.322 90(5)	0.203 86(4)	0.2878(2)	1.0	0.0076(15)
C3	0.342 91(7)	0.220 40(4)	0.0916(2)	1.0	0.0076
C4	0.353 35(8)	0.183 20(6)	−0.029 48(10)	1.0	0.0076
H8	0.3689(2)	0.196 05(11)	−0.1818 (2)	1.0	0.0099
C10	0.311 68(11)	0.243 86(9)	0.4180(3)	1.0	0.0137(12)
O11	0.320 32(14)	0.292 30(9)	0.3504(5)	1.0	0.0137
O12	0.2936(2)	0.2289 (1)	0.5949(3)	1.0	0.0137
O16	0.3522(2)	0.272 43(7)	0.0190(5)	1.0	0.0137
O18	0.2212(5)	0.2135(3)	−0.0316(10)	1.0	0.0798(15)
Oxygens (of water molecules in channels, hydrogens not located)					
O20	0.4732(3)	0.1114(3)	−0.0357(10)	1.0	0.0798
O21	0.0484(6)	−0.0124(6)	0.1349(13)	0.598(6)0.0798	
O22	0.1808(3)	0.5646(3)	0.1605(11)	0.934(7)0.0798	
O23	0.1578(4)	0.0723(4)	0.1161(14)	0.760(7)0.0798	

https://doi.org/10.1017/S0885715612000863 Published online by Cambridge University Press

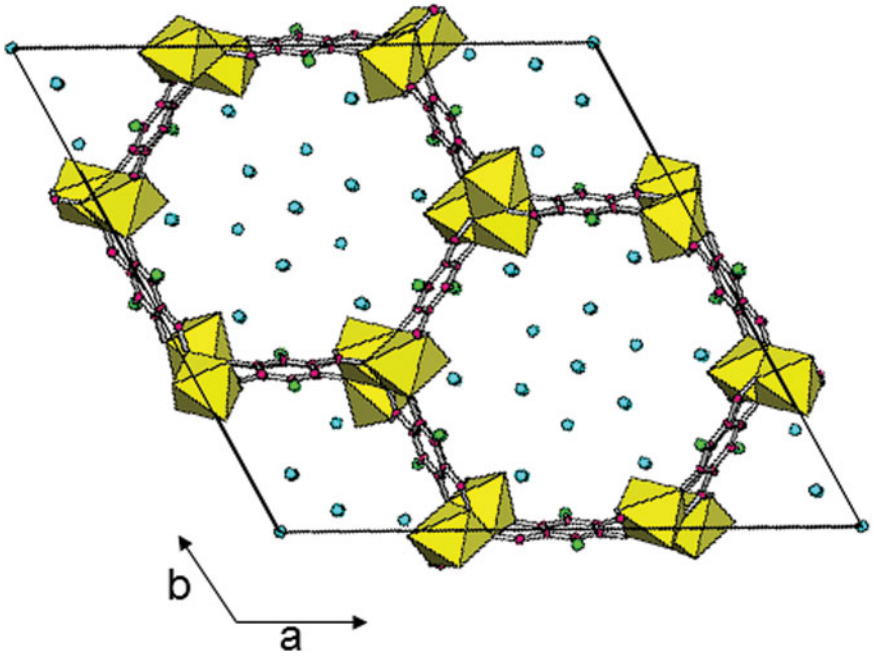

Figure 2. The [001] view of the structure of M_2(dhtp) (M = Mn and Ni), showing the large one-dimensional channel pore with partially occupied water molecules (only oxygen atoms are shown). The MO_6 groups are represented with yellow octahedra (blue sphere, oxygen; red spheres, C; green spheres, H).

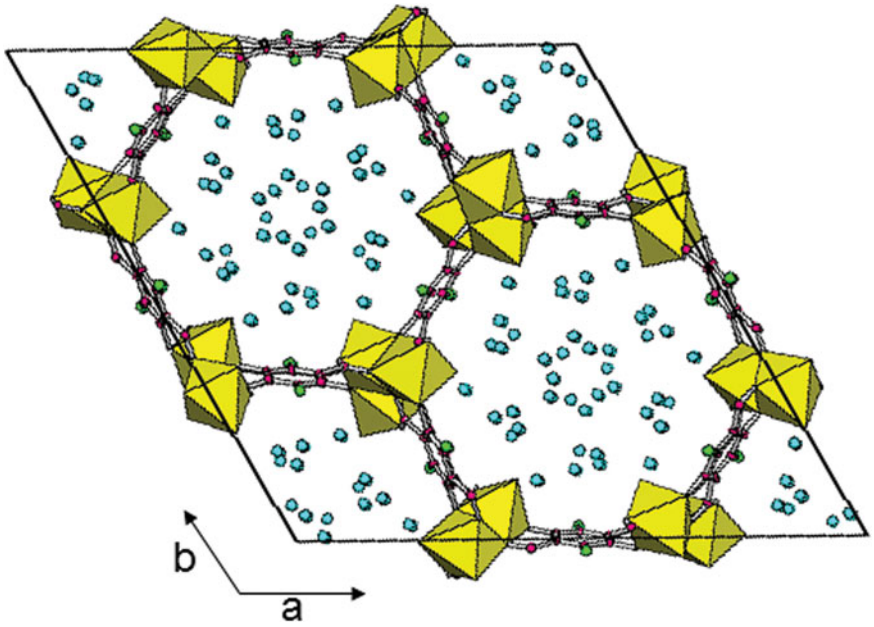

Figure 3. The [001] view of the structure of M_2(dhtp) (M = Co), showing the large one-dimensional channel pore with partially occupied water molecules (only oxygen atoms are shown). The CoO_6 groups are represented with yellow octahedra (blue sphere, oxygen; red spheres, C; green spheres, H).

The V_b values for the Mn-, Co-, Ni-, and Zn-analogs around the M sites were calculated to be 2.212, 1.950, 2.077, and 2.234, respectively. The V_b values for all four M–O octahedral sites indicate that they are all of 2+ ion. Although Co^{2+} is under tensile stress or underbonding (in an over-sized cage environment) as V_b values (1.950) are smaller than the ideal valence of 2+ for that site, the V_b of Mn^{2+}, Ni^{2+}, and Zn^{2+} are all greater than the value of 2 indicating that they are under compressive stress. As these are isostructural analogs, one possible explanation is that as the Co phase has substantially more water molecules in the channels, there are possible weak intermolecular interactions such as hydrogen bondings between the octahedral apexes (oxygen sites) with the water molecules, giving rise to tensile strain to the octahedral cage.

B. High-resolution X-ray powder diffraction pattern

The high-resolution reference pattern of a representative Mn-MOF74 is given in Table V as an example. In this pattern, the symbols 'M' and '+' refer to peaks containing contributions from two and more than two reflections, respectively. The symbol * indicates that the particular peak has the strongest intensity of the entire pattern and has been designated a value of '999'. The intensity values reported are integrated intensities rather than peak heights. This pattern has been submitted for inclusion in the Powder Diffraction File (PDF).

IV. Summary

The M_2(2,5-dihydroxytetephthalate) (M = Ni-, Co-, Mn-, and Zn-) or the MOF74 family of compounds provide more

https://doi.org/10.1017/S0885715612000863 Published online by Cambridge University Press

TABLE IV. Relevant bond distances found in M_2(dhtp), M = Mn, Co, Ni, Zn. Rigid body distances in the organic moiety have been employed.

Bonds	Bond distances (Å)			
	Mn	Co	Ni	Zn
MO_6 Octahedron				
M-O11	2.382(4)	2.089(4)	2.138(4)	2.122(3)
M-O12	2.006(2)	2.075(4)	1.938(2)	1.959(2)
M-O16	2.098(3)	2.044(4)	2.050(4)	1.985(2)
M-O16	2.048(3)	2.040(5)	1.856(3)	2.049(3)
M-O11	2.434(2)	2.265(5)	2.151(2)	2.2915(2)
M-O18	2.185(11)	2.185(5)	2.333(2)	2.100(7)
Organic (carboxylate)rigid body				
C2-C3	1.392	1.392	1.392	1.392
C2-C10	1.497	1.539(5)	1.497	1.497
C3-C4	1.392	1.392	1.392	1.392
C3-O16	1.348	1.377(4)	1.348	1.348
C4-H8	1.081	1.0811	1.081	1.081
C10-O11	1.255	1.187(7)	1.255	1.255
C10-O12	1.255	1.195(6)	1.255	1.255

insight into the chemistry of materials which possess coordinatively unsaturated open metal sites and small cylindrical pores. A brief comparison of the structure in terms of relevant bond distances and bond angles around the MO_6 octahedral coordination environment of the metal ion shows that four of the M–O distances are shorter than the other two. The water molecule (M–O18) is *trans* to the longest M–O bond, and its M–O18 distance is also elongated. The bond valence calculations illustrate that while the V_b values for the M = Mn, Ni and Zn compounds are all over the value of 2 (compressive stress), the corresponding value for the Co-analog was found to be <2 (tensile stress). In Co-MOF74, the interactions of the coordinated oxygen sites with the larger number of water molecules (hydrogen bonding

TABLE V. X-ray diffraction pattern for Ni_2(dhtp), (Trigonal R $\bar{3}$, a = 25.8561 (4) Å and c = 6.7119(2) Å, Z = 3). The symbols 'M' and ' + ' refer to peaks containing contributions from two and more than two reflections, respectively. The symbol * indicates that the particular peak has the strongest intensity of the entire pattern and is designated a value of '999'.

d	*I*	*h*	*k*	*l*	*d*	*I*	*h*	*k*	*l*	*d*	*I*	*h*	*k*	*l*
12.928	999	1	1	0	7.4642	543	3	0	0	6.4297	19	1	0	1
5.7570	8	2	0	−1	5.2592	71	3	−1	1 M	5.2592	71	2	1	1 M
4.8864	56	4	1	0	4.5586	20	4	−1	−1 M	4.5586	20	3	1	−1 M
4.2992	2	4	0	1	4.0795	43	3	2	1 M	4.0795	43	5	−2	1 M
3.7321	10	6	0	0	3.5812	50	6	−2	−1 +	3.4500	89	6	−1	1 M
3.4500	89	5	1	1 M	3.2278	27	7	−3	1	3.1198	30	3	−1	−2 M
3.1198	30	2	1	−2 M	3.0436	9	6	1	−1	2.9660	34	7	1	0
2.9526	3	4	−1	2	2.8822	15	5	3	−1 M	2.8822	15	4	0	−2 M
2.8157	101	8	−2	1 +	2.6296	14	6	−2	2	2.5768	61	6	−1	−2 M
2.5768	61	5	1	−2 M	2.5334	10	9	−2	−1 +	2.4802	21	4	3	−2 +
2.4419	33	9	−1	1 +	2.3983	8	6	4	−1 +	2.3587	13	7	3	1 M
2.3587	13	10	−3	1 M	2.3220	5	11	−4	0	2.3156	23	7	0	−2 M
2.3156	23	8	−3	2 M	2.2793	13	8	−2	−2 M	2.2793	13	6	2	−2 M
2.2158	8	9	1	−1 M	2.2158	8	11	−5	1 M	2.2047	7	1	1	3M
2.2047	7	1	1	−3 M	2.1799	71	5	4	−2	2.1445	25	3	0	3 +
2.1197	60	9	−2	2 +	2.0961	10	11	−2	1	2.0660	49	8	1	−2 +
2.0384	32	10	−4	2 +	2.0148	26	7	3	−2 +	1.9858	11	3	3	−3 M
1.9858	11	3	3	3 M	1.9244	10	9	1	2 +	1.9006	18	7	−2	3 +
1.8824	6	8	3	2 M	1.8824	6	11	−3	2 M	1.8637	17	10	0	−2 +
1.8469	13	7	7	0 +	1.8437	10	11	−2	−2 +	1.8073	13	12	−5	2
1.7912	24	8	4	−2 +	1.7405	2	11	0	2	1.7098	3	7	6	−2
1.6807	8	11	1	−2	1.6671	11	13	0	1 +	1.6525	13	14	−1	0 +
1.6427	14	10	5	−1 +	1.6200	3	3	1	−4	1.6112	14	11	−4	−3 +
1.5599	8	6	−2	−4	1.5487	9	5	1	4	1.5422	5	11	−1	3 +
1.5324	4	15	−7	−2 +	1.5195	5	12	−3	3	1.5129	8	12	4	−1 +
1.5114	4	10	5	2	1.4860	5	8	−3	−4 +	1.4912	11	13	−5	−3 +
1.4763	10	6	2	4 +	1.4546	5	17	−4	0	1.4483	8	5	4	4
1.4337	7	13	2	2 +	1.4243	8	7	7	−3 +	1.4132	9	8	1	4
1.3999	11	14	−4	3 +	1.3654	15	13	5	−1 +	1.3357	9	9	2	4 +
1.3201	6	12	−5	−4 +	1.3148	8	8	4	4 +	1.2796	4	6	−2	5 +
1.2612	5	4	3	−5	1.2379	4	7	0	−5					

https://doi.org/10.1017/S0885715612000863 Published online by Cambridge University Press

network) may contribute to this difference. The reference X-ray powder diffraction patterns of these compounds have been submitted for inclusion in the Powder Diffraction File (PDF).

ACKNOWLEDGEMENTS

Use of the Advanced Photon Source at the Argonne National Laboratory was supported by the U. S. Department of Energy, Office of Science, Office of Basic Energy Sciences, under Contract No. DE-AC02-06CH11357. This work utilized facilities supported in part by the National Science Foundation under Agreement No. DMR-0454672. Partial support by ICDD (Grant-in-Aid 09-03) is also acknowledged.

Brese, N. E. and O'Keeffe, M. (**1991**). "Bond-valence parameters for solids," Acta Crystallogr. *B* **47**, 192–197.

Britt, D., Furukawa, H., Wang, B., Glover, T. G., and Yaghi, O. M. (**2009**). "Highly efficient separation of carbon dioxide by a metal-organic framework replete with open metal sites," Proc. Natl. Acad. Sci. U.S.A. **106** (49), 20637–20640.

Brown, I. D. and Altermatt, D. (**1985**). "Bond-valence parameters obtained from a systematic analysis of the inorganic crystal structure database," Acta Crystallogr. *B* **41**, 244–247.

Caskey, S. R., Wong-Foy, A. G., and Matzger, A. J. (**2008**). "Dramatic tuning of carbon dioxide uptake via metal substitution in a coordination polymer with cylindrical pores," J. Am. Chem. Soc. 130, 10870–10871.

Dalesio, L. R., Hill, J. O., Kraimer, M., Lewis, S., Murray, D., Hunt, S., Watson, W., Clausen, M., and Dalesio, J. (**1994**). "The experimental physics and industrial control-system architecture-past, present, and future," Nucl. Instrum. Methods Phys. Res. A **352**, 179–184.

Dietzel, P. D. C., Morita, Y., Blom, R., and Fjellvåg, H. (**2005**). "An *in situ* high-temperature single-crystal investigation of a dehydrated metal-organic framework compound and field-induced magnetization of one-dimensional metal-oxygen chains," Angew. Chem. Int. Ed. **44**, 6354–6358.

Dietzel, P. D. C., Panella, B., Hirscher, M., Blom, R., and Fjellvåg, H. (**2006**). "Hydrogen adsorption in a nickel based coordination polymer with open metal sites in the cylindrical cavities of the desolvated framework," Chem. Commun., 959–961.

Glover, T. G., Peterson, G. W., Schindler, B. J., Britt, D., and Yaghi, O. (**2011**). "MOF74 building unit has a direct impact on toxic gas adsorption," Chem. Eng. Sci. **66**, 163–170.

Larson, A. C. and von Dreele, R. B. (**1992**). "GSAS-General Structure Analysis System," US Government contract (W-7405-ENG-36) by the Los Alamos National Laboratory, which is operated by the University of California for the U.S. Department of Energy.

Lee, P. L., Shu, D., Ramanathan, M., Preissner, C., Wang, J., Beno, M. A., Von Dreele, R. B., Lynn Ribaud, Kurtz, C., Antao, S. M., Jiao, X., and Toby, B. H. (**2008**). "A twelve-analyzer detector system for high-resolution powder diffraction," J. Synchrotron Radiat., **15**, 427–432.

PDF, Powder Diffraction File, ICDD, Newtown Squares, PA

Rietveld, H. M. (**1969**). "A profile refinement method for nuclear and magnetic structures," J. Appl. Crystallogr. **2**, 65–71.

Rosi, N. L., Kim, J., Eddaoudi, M., Chen, B., O'Keeffe, M., and Yaghi, O. M. (**2005**). "Rod packings and metal-organic frameworks constructed from R-d-shaped secondary building units," J. Am. Chem. Soc. **127**, 1504–1518.

Shannon, R. D. (**1976**). "Revised Effective Ionic Radii and Systematic Studies of Interatomie Distances in Halides and Chaleogenides," Acta Crystallogr. **A32**, 751–767.

Standard reference materials (SRMTM) are produced by National Institute of Standards SRM Office, Gaithersburg, MD 20899. For details, please contact srminfo@nist.gov.

Tranchemontagne, D. J., Hunt, J. R., and Yaghi, O. M. (**2008**). "Room temperature synthesis of metal-organic framework: MOF-5, MOF-74, MOF-177, MOF-199, and IRMOF-0," Tetrahedron **64**, 8553–8557.

Wang, J., Toby, B. H., Lee, P. L., Ribaud, L., Antao, S., Kurtz, C., Ramanathan, M., Von Dreele, R. B., and Beno, M. A. (**2008**). "A dedicated powder diffraction beamline at the advanced photon source: commissioning and early operation results," Rev. Sci. Instrum. **79**, 085105.

Wu, H., Zhou, W., and Yildirim, T. (**2009**). "High-capacity methane storage in metal-organic frameworks M_2(dhtp): the important role of open metal sites," J. Am. Chem. Soc. **131**, 4995–5000.

Wu, H., Simmons, J. M., Srinivas, G., Zhou, W., and Yildirim, T. (**2010**). "Adsorption sites and binding nature of CO_2 in prototypical metal-organic frameworks" A combined neutron diffraction and first-principles study," J. Phys. Chem. Lett. **1**, 1946–1951.

Zhou, W., Wu, H., and Yildirim, T. (**2008**). "Enhanced H_2 Adsorption in isostructural metal-organic frameworks with open metal sites: strong dependence of the binding strength on metal ions," J. Am. Chem. Soc. **130**, 15368–15269.